

CHAPTER III

STRUCTURE AND PHASE DIAGRAM OF OXIDE SUPERCONDUCTORS

The single most important experiment to be performed on a new copper-oxide superconducting material is to determine its crystal structure. Virtually no serious conjecture as to the properties of a compound can be made without this knowledge and as soon as the structure of a novel material is established, a number of models for their properties will appear. The purpose of this chapter is to give an overview of the structural studies performed on these superconducting oxides. Since it is paramount that these structures be understood clearly, we shall present here the structural information on the $\text{La}_{2-x}\text{M}_x\text{CuO}_{4-y}$ and $\text{YBa}_2\text{Cu}_3\text{O}_{7-\delta}$ systems in detail and provide a brief description of the large number of superconducting structures that exist in the Bi- and Tl-based oxides. The phase diagrams for these oxide superconductors are discussed in the last section.

Structure of La-M-Cu-O the system

Bednorz and Müller [7], first discovered high temperature superconductivity in barium-doped lanthanum in the copper-oxide compounds. The superconductivity component of the compound mixture was later identified as having the stoichiometry $\text{La}_{2-x}\text{Ba}_x\text{CuO}_{4-y}$. Similar materials have been studied extensively, and similar results have been obtained in $\text{La}_{2-x}\text{M}_x\text{CuO}_{4-y}$ with $\text{M} = \text{Ba}, \text{Ca}$ and Sr , where Sr yields the highest T_c (on the order of 40 K, for x near 0.15 [47]). At high temperatures all of the La214 copper oxides exhibit the body-center tetragonal K_2NiF_4 structure (see Fig. 6a). This structure is made by stacking alternate layers of perovskite, LaCuO_3 and rock salt, LaO , along the c -axis such that the copper sites of one perovskite layer are aligned with the lanthanum sites in the next perovskite layer (see Fig. 6b).

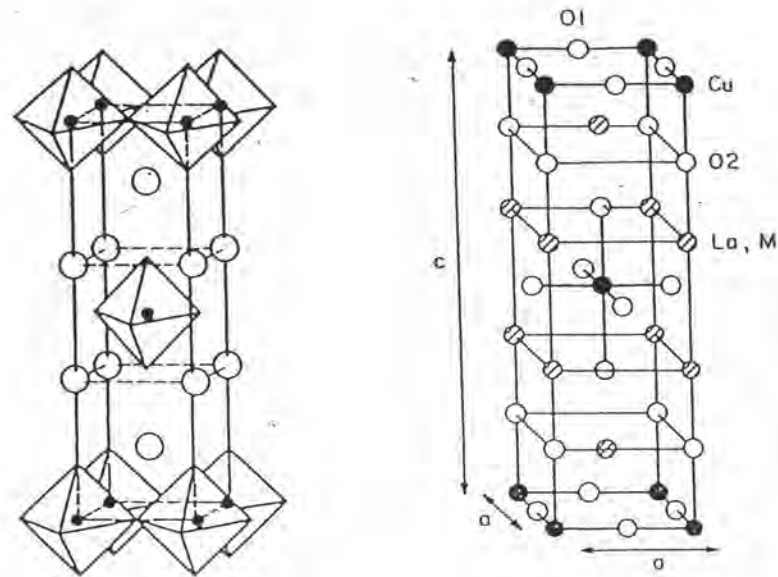
(6a) K_2NiF_4 structure(6b) $\text{La}_{2-x}\text{M}_x\text{CuO}_{4-y}$ structure

Fig. 6 The K_2NiF_4 perovskite structure and the body-centered tetragonal structure of $\text{La}_{2-x}\text{M}_x\text{CuO}_{4-y}$.

There is a tetragonal to orthorhombic phase transition, which occurs in the $\text{La}_{2-x}\text{M}_x\text{CuO}_{4-y}$ structure with changes in the dopant concentration (x) and temperature. A general representation is presented in Fig. 7 which shows the copper-oxygen and ninefold lanthanum-and-strontium oxygen coordination of $\text{La}_{1.85}\text{Sr}_{0.15}\text{CuO}_4$ at 10 K. On the scale of the figure, the orthorhombic and tetragonal structures are not distinguishable. The perovskite planes of CuO_6 octahedra are emphasized to illustrate the highly two-dimensional nature of the plane (perpendicular to c) in which the strong copper-oxygen [O(2)] orbital overlap occurs. These copper-oxygen planes are separated by planes of (La and Sr)-O(1). The copper atoms in one plane do not share oxygen with copper atoms in other planes. The oxygen atoms in the copper-oxygen plane [O(2)] are bonded to two copper atoms within the planes, and also to four La and Sr atoms in an adjacent plane.

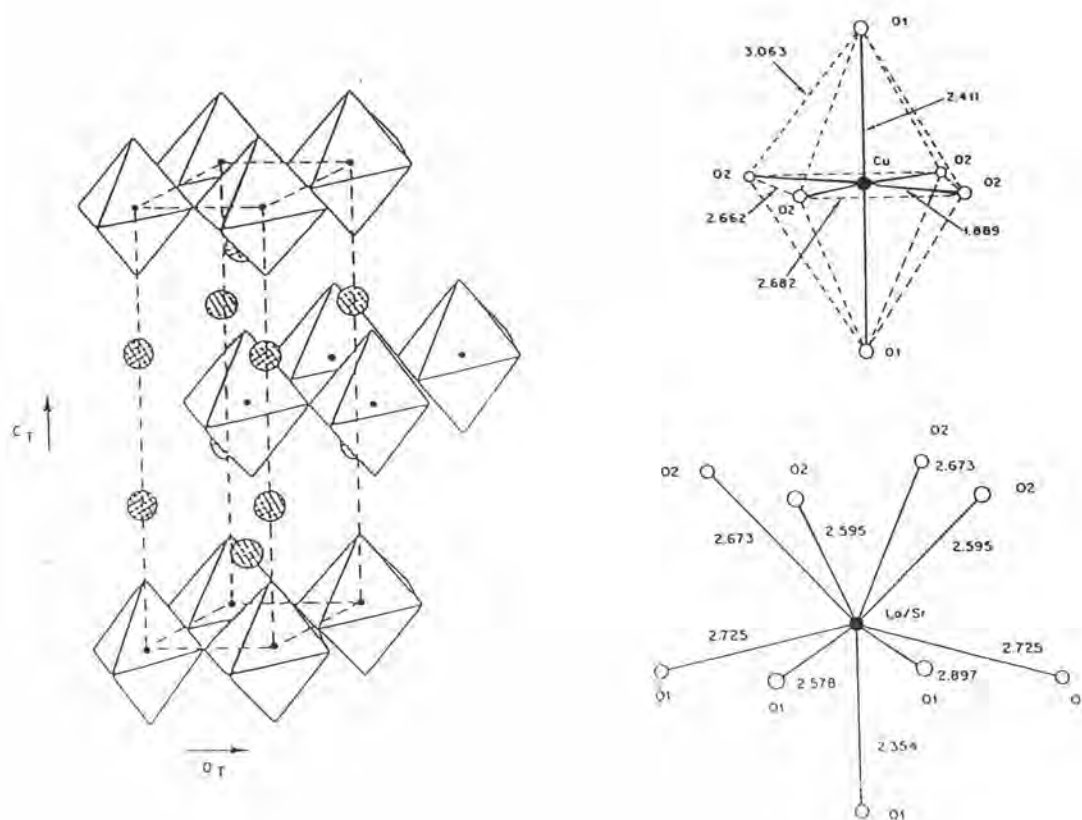


Fig. 7 General view of the highly two-dimensional tetragonal $\text{La}_{2-x}\text{M}_x\text{CuO}_{4-y}$ structure, the CuO_6 octahedra and the ninefold of Sr and La coordinations. The La and Sr atoms, large shaded circles; Cu atoms, small filled circles. Oxygen atoms at vertices of polyhedra: O(2) atoms are at vertices within the Cu-O planes (perpendicular to c), O(2) atoms at the vertices between these planes.

In Fig. 7 lanthanum and strontium are nine-coordinated to oxygen in both the tetragonal and orthorhombic structures. The shape of the polyhedron is that of a square antiprism with one copper face, with the La and Sr displaced considerably from the antiprism center towards the copper face. The La and Sr-O(1) "plane" is perpendicular

to the c-axis. The La and Sr atoms need to occupy exactly the same position on this polyhedron. The La and Sr atoms are equally strongly bonded to the oxygen atoms but only weakly bonded to Cu [O(1)] and those involved in the Cu-O conducting plane [O(2)]. Thus the nature of the atom on this site may strongly influence the Cu-O(2) bonding. This suggests a microscopic reason for the strong influence of the La site substitution on T_c . The shape of the La and Sr oxygen polyhedra is somewhat different in the tetragonal and orthorhombic structures with two bond lengths to [O(1)] considerably altered. Bond lengths to O(2) atoms are also different but the average (La and Sr)-O bond length seems only to decrease smoothly with temperature. There is no change in the La and Sr oxygen coordination at T_c . The interatomic separation and angles for these polyhedra are shown in Table 1[47].

Table 1 Bond lengths and angles in the copper-oxygen polyhedron and metal-oxygen bond in $\text{La}_{1.85}\text{Sr}_{0.15}\text{CuO}_4$.

	300 K	60 K	10 K
Cu - O(1) (x 2)	2.4124	2.4110	2.4112
Cu - O(2) (x 4)	1.8896	1.8894	1.8893
O(2) - O(2) (x 4)	2.6723		
(x 2)		2.6814	2.6816
(x 2)		2.6626	2.6620
O(2) - O(1) (x 4)	3.0644	3.063	3.063
Cu - Cu	3.7793	3.7759	3.7755
O(2) - Cu - O(2)	90.0	89.58	89.58
		90.42	90.42
O(2) - Cu - O(1)	90.0	89.9	89.9
Cu - O(2) - Cu	180.0	175.4	175.4
La - O(1) (x 1)	2.3557	2.3545	2.3545
(x 4)	2.732		
(x 2)		2.7253	2.7250
(x 1)		2.5776	2.5784
(x 1)		2.8978	2.897
- O(2) (x 4)	2.6409		
(x 2)		2.597	2.595
(x 2)		2.6726	2.6731
Average La - O	2.650	2.647	2.646

The precise structure and resulting properties of $\text{La}_{2-x}\text{M}_x\text{CuO}_{4-y}$ depend sensitively on processing. Many of the early studies [7, 47-50] examined the effects of changing the alkaline earth dopant and its concentration. Superconducting transition temperatures of 37, 32, and 17 K were found for Sr, Ba and Cu respectively, for $x \sim 0.15$ [7]. It rapidly became evident, however, that oxygen and lanthanum deficiencies also affect superconducting properties. This point was brought out in studies of undoped $\text{La}_{2-x}\text{CuO}_{4-y}$, which can be either a 40 K[51] superconductor or an antiferromagnetic insulator[32-35], depending on the lanthanum and oxygen concentrations.

Structure of the Y-Ba-Cu-O system

Soon after the discovery and confirmation of superconductivity in the Y-Ba-Cu-O system [3, 52, 53], the phase responsible for the 90 K transition temperature was found to have a cation stoichiometry of $1\text{Y} : 2\text{Ba} : 3\text{Cu}$. The unit cell dimensions determined by electron and x-ray diffraction identified the structure as being related to a cubic perovskite with one of the cubic axes tripled [54-58] (see Fig. 8b). In the basic perovskite structure ABX_3 (see Fig. 8a), there are two cation sites. An A ion site lies at the centers of a cage formed by corner-sharing anion octahedra and accommodates the larger cations in the structure. The B ion site lies at the centers of the anion octahedra and accommodates the smaller cations. It was therefore natural to place the larger Y and Ba ions on the A sites and the smaller Cu ions in the B sites. The tripling of the perovskite unit cell could then be accounted for by ordering the Y and Ba ions on the A sites such that the top and bottom cells are in a stack of three containing Ba ions, while the middle cell contains a Y ion. This basic cation arrangement was not only consistent with the $1\text{Y} : 2\text{Ba} : 3\text{Cu}$ stoichiometry but also provided a reasonable fit to x-ray powder diffraction data [54-57] obtained from nearly single-phase materials.

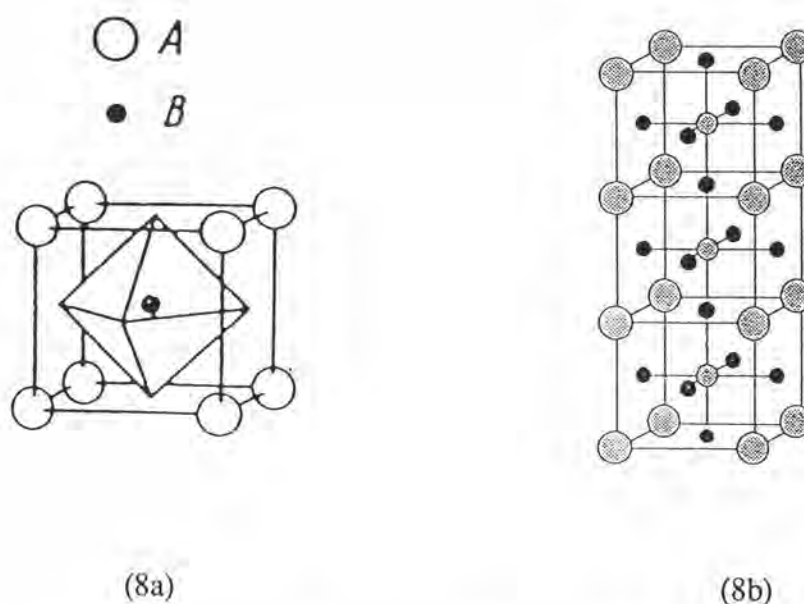


Fig. 8 The ABO_3 perovskite structure(8a), and the stack of three perovskite cell (8b).

There are 3 anions per unit cell in the ideal perovskite structure, corresponding to 3 possible oxygen sites in a triple perovskite unit cell. Formal balancing of the charges on the cations requires a maximum of 8 oxygen atoms per unit cell and the copper atom is assumed to be in a +3 state, with 6.5 and 5 oxygen ions per unit cell if charges of +2 and +1 are assumed for all the copper cations. X-ray diffraction from small single crystals extracted from sintered polycrystalline material confirmed that it was therefore clear that the Y123 structure was oxygen deficient relative to the ideal perovskite structure. The x-ray data [56-57] showed that the Y ion was surrounded by 8 oxygen ions rather than by 12 ions as in the ideal perovskite structure. Oxygen deficiency was also noted in the basal copper plane between the Ba ion. Anion sites in this plane, which lie along the cell edges, were found to be only half occupied.

Refinements of the cell parameters studied by Seigrest [59] indicated that the unit cell was orthorhombic with b slightly larger than a , even though some single crystal studies observed a tetragonal distribution of diffraction intensities. The essential features of the orthorhombic structures are shown in Fig. 9. The effect of oxygen

ordering in the basal plane of the structure is to occupy one of the oxygen sites along a cell edge and to leave the other site vacant. The cell edge with the occupied site, produces an orthorhombic unit cell. The ordering puts the copper ions in the basal plane of the structure, at the center of square arrangements of copper and oxygen ions linked together by sharing their corners to form "linear chains" along the basis of the structure. A recent neutron diffraction study [60] suggests that the chain may not be perfectly lined. The effect of vacant oxygen sites around the Y ion can also be seen in the figure. The absence of oxygen from the Y plane places the copper ions in a square pyramidal structure. Linking of the square bases of the pyramids at their corners results in two-dimension of procured sheets of copper-oxygen bonds that are external in the a-b plane of the structure. The chains and planes in the structure are linked through the oxygen atoms that lie at the apices of the square pyramids.

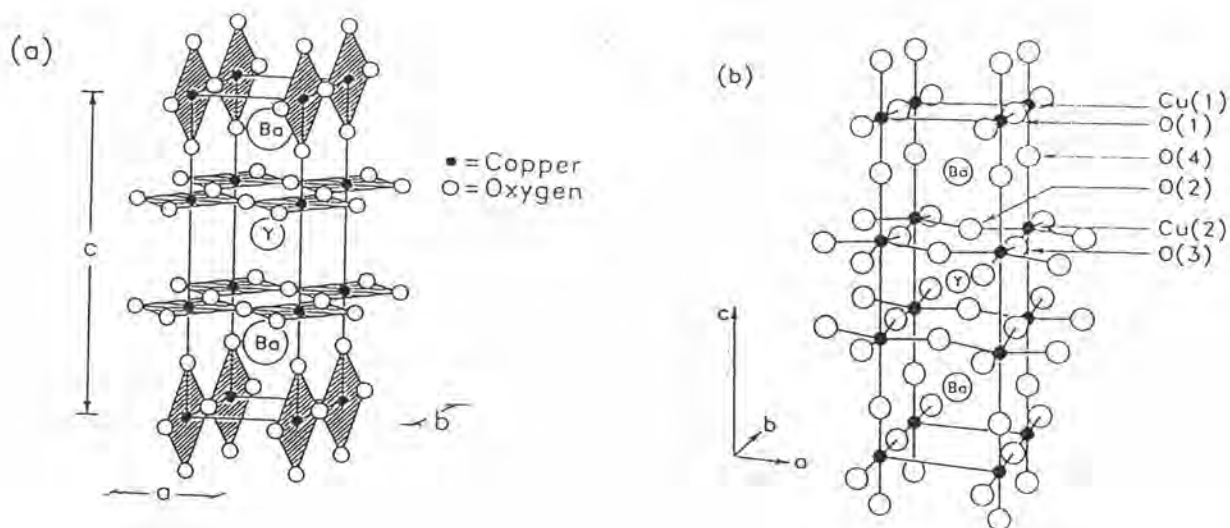


Fig. 9 The structure of $\text{YBa}_2\text{Cu}_3\text{O}_{7.8}$, the coordination of copper with oxygen is emphasized to show the location of copper-oxygen planes and chains.

Table 2 Selected bond lengths(Å) and angles (Å) in orthorhombic YBa₂Cu₃O₇.

bound length (Å)		angle (Å)	bound length (Å)	
Y - O(2)	4 x 2.418		Cu(1) - O(1)	2 x 1.947
Y - O(3)	4 x 2.399		Cu(1) - O(4)	2 x 1.834
Ba - O(1)	2 x 21.891		Cu(2) - O(2)	2 x 1.929
Ba - O(2)	2 x 2.980		Cu(2) - O(3)	2 x 1.961
Ba - O(3)	2 x 2.984		Cu(2) - O(4)	2.341
Ba - O(4)	4 x 2.750			
O(1) - Cu(1) - O(4)		90.0		
O(4) - Cu(1) - O(4)		180.0		
O(1) - Cu(1) - O(1)		180.0		
O(3) - Cu(2) - O(3)		166.3		
O(2) - Cu(2) - O(2)		165.3		
O(2) - Cu(2) - O(3)		89.1		
O(4) - Cu(2) - O(3)		96.9		
O(4) - Cu(2) - O(2)		97.4		

Selected bond lengths and angles for the structure are given in Table 2[59]. The Y-O and Ba-O distances are typical and compare well with distances observed in other structures. The Cu(2)-O(2) and Cu(2)-O(3) distances in the planes are 1.929 Å and 1.961Å, respectively whereas the Cu(2)-O(4) bond, joins the copper atom in the plane to the apical O(4) atom. The Cu(2)-O(4) distance suggests that the copper atoms in the planes are only weakly linked to those in the chains via the apical oxygen. It has been suggested that the short Cu(1)-O(4) bond distance is a consequence of the preferential location of Cu³⁺ ions in the chain sites.

The oxygen content in the 123 structure depends strongly on the processing[61-63] conditions used to form the material. An YBa₂Cu₃O₇ stoichiometry is only reached if samples are slowly cooled in oxygen. Quenching from high temperatures or cooling in a reducing atmosphere results in a more oxygen deficient structure. If sufficient oxygen is removed, the structure undergoes an orthorhombic-to-tetragonal phase

transformation. Rietveld refinements of neutron diffraction data taken from oxygen deficient materials show that oxygen is lost primarily from the O(1) site in the chains. In a reduced material with six oxygen atoms per unit cell the chain site is completely empty, which reduces the coordination of the Cu(1) atom to two.

Bismuth-Containing Superconductors

In May 1987, Michel [64] reported the discovery of superconductivity with transition temperatures between 7 and 22 K in the Bi-Sr-Cu-O system. Because of the intense interest in the 90 K materials at that time, their report did not attract widespread interest. However, attention quickly focussed on the bismuth-containing superconductors in January 1988 when Maeda and Chu [5] reported that adding Ca to the Bi-Sr-Cu-O system produced a material that was superconducting above liquid nitrogen temperatures. Three superconducting oxides were subsequently identified in the Bi-Ca-Sr-Cu-O system. $\text{Bi}_2\text{Sr}_2\text{Cu}_1\text{O}_{6+x}$ ($T_c = 7-22$ K), $\text{Bi}_2\text{Ca}_1\text{Sr}_2\text{Cu}_2\text{O}_{8+x}$ ($T_c \sim 85$ K), and $\text{Bi}_2\text{Ca}_2\text{Sr}_2\text{Cu}_3\text{O}_{10+x}$ ($T_c \sim 110$ K). For brevity, these phases will be referred to as Bi2021, Bi2122, and Bi2223, respectively. The structures consisted of perovskite-like units containing one, two, or three CuO_2 planes sandwiched between Bi-O bilayers (Fig. 10d, e and f). Bi2021 is responsible for the results reported by Michel [64] and remains the least studied of the three because of its low transition temperature. Bi2122 has been the most extensively studied bismuth-containing superconductor. The perovskite-like unit in Bi2122 is remarkably similar to that in Y123, the Ca and Sr cations in Bi2122 playing the same role as the Y and Ba cations in Y123 structure. The linear chains in the Y123 structure are replaced by the Bi-O layers, but these layers are not essential for high-temperature superconductivity. The processing conditions required to form a single phase or a single crystal of Bi2223 have yet to be determined[5, 65]. Consequently, the structure and properties of this phase have not been studied extensively. The first

Bi-Ca-Sr-Cu-O samples displayed sharp drops in resistance at around 110 K, but did not reach zero resistance above 100 K [5]. Susceptibility measurements indicated that two superconducting transitions were present in most samples, one at 85 K and the other at 110 K. Subsequent studies [66] identified Bi2122 as the 85 K phase and linked the 110 K transition to the presence of the Bi2223 phase. The connectivity between Bi2223 grains appears to be quite poor, because it is difficult to reach zero resistance at 110 K even in samples in which Bi2223 is the predominant phase. Unless the difficulties in preparing Bi2223 can be overcome, there is little chance for scientific or technical progress in studies of this phase.

Thallium-Containing Superconductors

Sheng and Hermann[67] discovered superconductivity above liquid nitrogen temperatures in the Tl-Ba-Cu-O system in January 1988. It was initially overshadowed by the breakthroughs in the Bi-Ca-Sr-Cu-O system. While numerous researchers struggled to achieve zero resistivity above 110 K in the bismuth system, Sheng and Hermann added Ca to their system and produced a Tl-Ca-Ba-Cu-O mixture that reached zero resistance at 107 K. This result sparked numerous investigations of the phases present in the Tl-Ca-Ba-Cu-O system. Two superconducting phases were identified in Sheng and Hermann's samples by Hazen[68], namely $\text{Tl}_2\text{Ca}_1\text{Ba}_2\text{Cu}_2\text{O}_{8+x}$ and $\text{Tl}_2\text{Ca}_1\text{Ba}_2\text{Cu}_2\text{O}_{10+x}$. Then Parkin [69] changed the processing conditions to greatly increase the amount of the $\text{Tl}_2\text{Ca}_1\text{Ba}_2\text{Cu}_2\text{O}_{10+x}$ phase and produced a material with bulk superconductivity at 125 K, the highest superconducting transition temperature yet found.

Six perovskite-related oxides have been identified in the Tl-Ca-Ba-Cu-O system so far, namely $\text{Tl}_1\text{Ba}_2\text{Cu}_1\text{O}_5$, $\text{Tl}_1\text{Ca}_1\text{Ba}_2\text{Cu}_2\text{O}_7$, $\text{Tl}_1\text{Ca}_2\text{Ba}_2\text{Cu}_3\text{O}_9$, $\text{Tl}_2\text{Ba}_2\text{Cu}_1\text{O}_6$, $\text{Tl}_2\text{Ca}_1\text{Ba}_2\text{Cu}_2\text{O}_8$, and $\text{Tl}_2\text{Ca}_2\text{Ba}_2\text{Cu}_3\text{O}_{10}$ (Fig. 10). These phases will be referred to as Tl1021, Tl1122, Tl1223, Tl2021, Tl2122, and Tl2223. Both the size and the

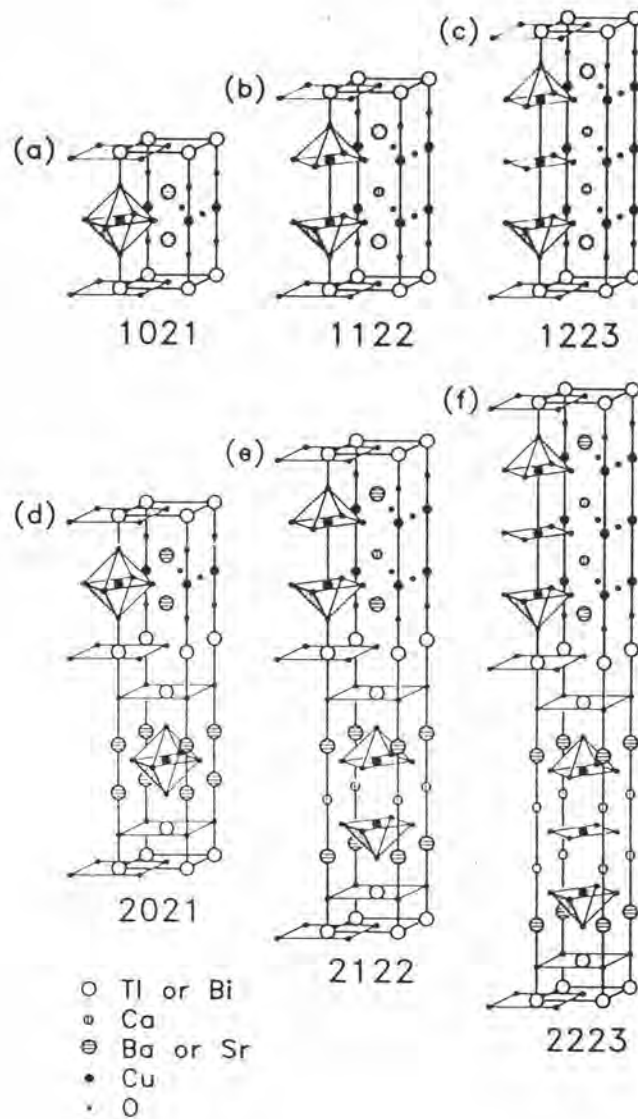


Fig. 10 Nominal unit cells for the bismuth- and thallium-containing superconductors : (a) $\text{Tl}_1\text{Ba}_2\text{Cu}_1\text{O}_5$, (b) $\text{Tl}_1\text{Ca}_1\text{Ba}_2\text{Cu}_2\text{O}_7$, (c) $\text{Tl}_1\text{Ca}_2\text{Ba}_2\text{Cu}_3\text{O}_9$, (d) $\text{Tl}_2\text{Ba}_2\text{Cu}_1\text{O}_6$, (e) $\text{Tl}_2\text{Ca}_1\text{Ba}_2\text{Cu}_2\text{O}_8$, (f) $\text{Tl}_2\text{Ca}_2\text{Ba}_2\text{Cu}_3\text{O}_{10}$. Only the 2021, 2122, and 2223 structures form in the Bi-based system, whereas all six structures form in the Tl-based system.

separation of the Cu perovskite-like units can be independently varied in the thallium-containing superconductors. Tl2021, Tl2122, and Tl2223 are made up of Cu perovskite-like units containing one, two, and three CuO_2 planes separated by Tl-O bilayers, respectively. They are thallium analogs to the nominal Bi2021, Bi2122, and Bi2223 structures. Conversely, Tl1021, Tl1122 and Tl1223 are made up of Cu perovskite-like units containing one, two, and three CuO_2 planes separated by Tl-O monolayers, respectively, and have no bismuth analogs.

Finally, all the superconducting cuprates have a perovskite related structure. The $\text{La}_{2-x}\text{M}_x\text{CuO}_4$ systems with the quasi two-dimensional K_2NiF_4 structure have a perovskite layer between two rock-salt layers. $\text{YBa}_2\text{Cu}_3\text{O}_{7-\delta}$ and related 123 compounds are defect perovskites. The new oxides of the Bi-Ca-Ba-Cu-O and Tl-Ca-Ba-Cu-O families conform to the general formula $\text{A}_2(\text{B},\text{B})_{n+1}\text{Cu}_n\text{O}_{2n+4}$, where B, B = Ca, Sr or Ba and A = Tl or Bi, and have structures comparable to those of the Aurivillius family of oxides, $\text{Bi}_2\text{O}_2(\text{A}_{n-1}\text{B}_n\text{O}_{3n+1})$, containing perovskite layers. All the cuprates have two-dimensional coordination of copper-oxygen layers which is essential in all the cuprates. Although orthorhombicity does not seem to be essential, most of the high T_c oxides are orthorhombic. All of the oxides have a tetragonal structure at room temperature. The oxides with Tl-O monolayers have primitive tetragonal cells, whereas the oxides with Tl-O bilayers have body-centered tetragonal cells. Tl2021 has two polymorphs, one face - centered orthorhombic and the other body-centered tetragonal.

Phase diagram

In this last section we would introduce the phase diagram [70] for the copper oxide superconductor. Besides the normal-superconducting phase transition, the new copper oxide materials show an unusually complex generalized phase diagram. The high-temperature phase of the La214 material is tetragonal. Studies of the temperature dependence of the crystal structure of La214 compounds reveal a tetragonal-to-

orthorhombic transition, reviving speculations about the connection between lattice instability and superconductivity. Magnetic susceptibility studies indicate a magnetic transition, probably involving antiferromagnetism, in some samples. The transition was found to be highly sensitive to the oxygen vacancy concentration which is easily varied in a ceramic polycrystalline sample by heat treatment. Initial studies suggested that antiferromagnetism did not occur in stoichiometric (the oxygen concentration $y = 0.00$) samples, but occurred with $y = 0.03$ and disappeared for y slightly larger. However, absolute oxygen concentrations are very difficult to establish on this scale, and, in addition, La substoichiometry is common in samples. These studies did serve to establish the extreme sensitivity of magnetic ordering to material parameters in the La214 system. Later, polarized neutron-diffraction studies established that antiferromagnetism does occur and the dependence of the Neel temperature T_N on the oxygen concentration y and the divalent metal concentration x has subsequently been established. It has become "common wisdom" that stoichiometric La214 with $x = 0$, and $y = 0$ is an antiferromagnet at low temperature although it is still questionable whether this "fact" has indeed been established by systematic studies of susceptibility on samples whose stoichiometry and crystalline perfection are established by Rietveld refinement of neutron diffraction data.

Due to the large crystalline, and therefore electronic, anisotropy in the layered materials, the question of metallic-nonmetallic character could be settled only with single crystal samples. Ceramic samples of undoped ($x = 0.00$) La214 showed extremely large resistivities which increase as the temperature was lowered, in nonmetallic fashion. However, individual measurements differ greatly, due to sample differences such as texturing, due to difficulties in establishing ohmic contacts, and to varying sample stoichiometries. Subsequent work on single crystals and Orion films did clarify that clean nonmetallic resistivities occurred for small x , which decrease rapidly with increasing x and become metallic below room temperature for x greater

than about 0.6. This behavior introduces yet another phase transition, a metal-insulator transition in the phase diagram. Thus in the La214 system there is a normal-superconducting transition, a tetragonal-to-orthorhombic structure transition, a paramagnetic-antiferromagnetic transition, and metal-insulator transition, all in the range $T < 500$ K, $x < 0.2$. A schematic representation of the phase diagram, is presented in Fig.11. Clearly there is an unusual assortment of competing chemical, magnetic, and thermal interactions in this system which provide a field rich for research.

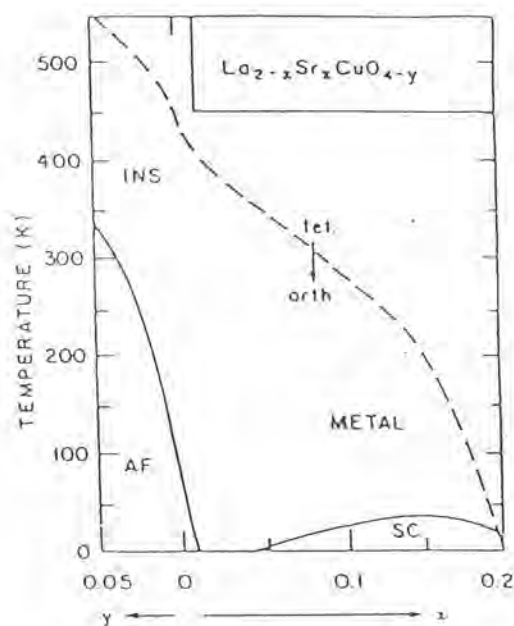


Fig. 11 Schematic phase diagram for $\text{La}_{2-x}\text{Sr}_x\text{CuO}_{4-y}$ [70].

The phase diagram for $\text{YBa}_2\text{Cu}_3\text{O}_{7-\delta}$ compounds, sketched in Fig. 12, is remarkably similar to that of the $\text{La}_{2-x}\text{Sr}_x\text{CuO}_{4-y}$ diagram. This compound also displays a wide range of behavior in its phase transformations. By increasing the hole concentration which is associated with a decreasing δ , the system again transforms from an antiferromagnet insulator to a metal that exhibits superconductivity at temperatures as high as 93 K ($\delta = 0$). An important complication is that, the structure

and properties of $\text{YBa}_2\text{Cu}_3\text{O}_{7-\delta}$ depend not only on δ but also on the distribution of O among a large number of possible sites. The variation from $\delta = 0$ to $\delta = 1$ affects only the O content of the Cu1-O1 layers. The results shown here were obtained under conditions in which, for $\delta < 0.7$, the Cu1-O1 chains remain largely intact with non-O sites along an axis perpendicular to the chains becoming occupied. An increase beyond $\delta = 0.7$ in the present case causes the remaining O in the Cu1-O1 layers to become equally distributed along the a and b axes. The symmetry thus changes at this point from orthorhombic to tetragonal symmetry.

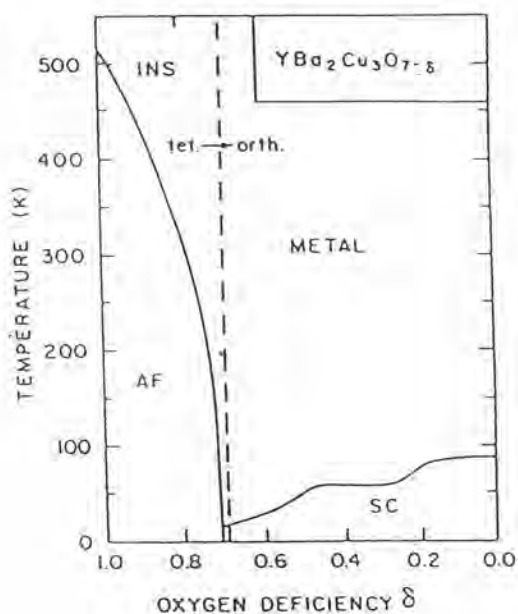


Fig. 12 Schematic phase diagram for $\text{YBa}_2\text{Cu}_3\text{O}_{7-\delta}$ based on experimental data [70].

This feature, as well as the incommensurate charge density wave feature of the Bi-based and Tl-based systems, clearly demonstrates that there is a great deal of unusual behavior in these Cu-O based systems, and there is a tendency to expect connections between any type of unexpected property and the unusually high transition temperature superconductors.